From the square lattice to the checkerboard lattice: Spin-wave and large-n limit analysis

Benjamin Canals*

Laboratoire Louis Néel, CNRS, 25 avenue des Martyrs, Boite Postale 166, 38042 Grenoble Cedex 9, France
(Received 20 November 2001; published 16 April 2002)

Within a spin wave analysis and a fermionic large-n limit, it is shown that the antiferromagnetic Heisenberg model on the checkerboard lattice may have different ground states, depending on the spin size S. Through an additional exchange interaction that corresponds to an intertetrahedra coupling, the stability of the Néel state has been explored for all cases from the square lattice to the isotropic checkerboard lattice. Away from the isotropic limit and within the linear spin-wave approximation, it is shown that there exists a critical coupling for which the local magnetization of the Néel state vanishes for any value of the spin S. One the other hand, using the Dyson-Maleev approximation, this result is valid only in the case $S = \frac{1}{2}$ and the limit between a stable and an unstable Néel state is at $S = 1$. For $S = \frac{1}{2}$, the fermionic large-n limit suggests that the ground state is a valence-bond solid build with disconnected four-spin singlets. This analysis indicates that for low spin and in the isotropic limit, the checkerboard antiferromagnet may be close to an instability between an ordered $S = 0$ ground state and a magnetized ground state.

I. INTRODUCTION

In one dimension (1D) the ground state of the Heisenberg antiferromagnet may be quasiordered or disordered, depending on the spin parity S.[1] When S is an integer and, in particular, when $S = 1$, the ground state corresponds to a magnetically disordered state where spin-spin correlation functions (CF's) exponentially decay with distance and with total spin $S_t = 0$. This state is called a quantum spin liquid (QSL) as the spin-spin CF's are equivalent to the density-density CF's in conventional liquids and because it has total spin $S = 0$ and no broken symmetry. This concept can be generalized to classical systems if the spins are considered as $O(3)$ vectors. The constraint $S = 0$ is then removed and the state is termed a classical spin-liquid (CSL). Another notion for spin-liquid ground states emerged from earlier studies by Wannier[2] and Houtappel[3] and is related to geometrical frustration. In that case, it is the geometry of the underlying lattice that leads to magnetic disorder and not its dimensionality. Naturally, frustrated structures may exist not only for $D = 1$ and for over 50 years frustrated lattices have been examined in the search for disordered ground states in higher dimensions ($D = 2,3$). One goal of this research into peculiar structures is the study of unconventional spectra, not covered by the Lieb-Mattis theorem.[4]

To date, two particular lattices have been considered as good candidates for spin-liquid ground states: the *kagomé* lattice and the pyrochlore lattice. The first one is a two-dimensional arrangement of corner sharing triangles, while the latter is a three-dimensional structure of corner sharing tetrahedra. Both lattices have been theoretically investigated and it has been suggested that in the classical case, as well as in the quantum case, they possess spin-liquid-like ground states.[5–8] Experimentally, all systems that can be well described by the antiferromagnetic Heisenberg model on these lattices have been found to possess this spin-liquid behavior or unconvential behaviors that can be ascribed in part to the underlying "theoretical" spin-liquid ground state.[9] This suggests that both the elementary cells (triangle or tetrahedron)

and the connectivity (corner sharing) are major ingredients for magnetic disorder. In this paper, we study such a lattice, where the elementary cell is a tetrahedron and where connectivity is corner sharing: the checkerboard lattice (see Fig. 1).
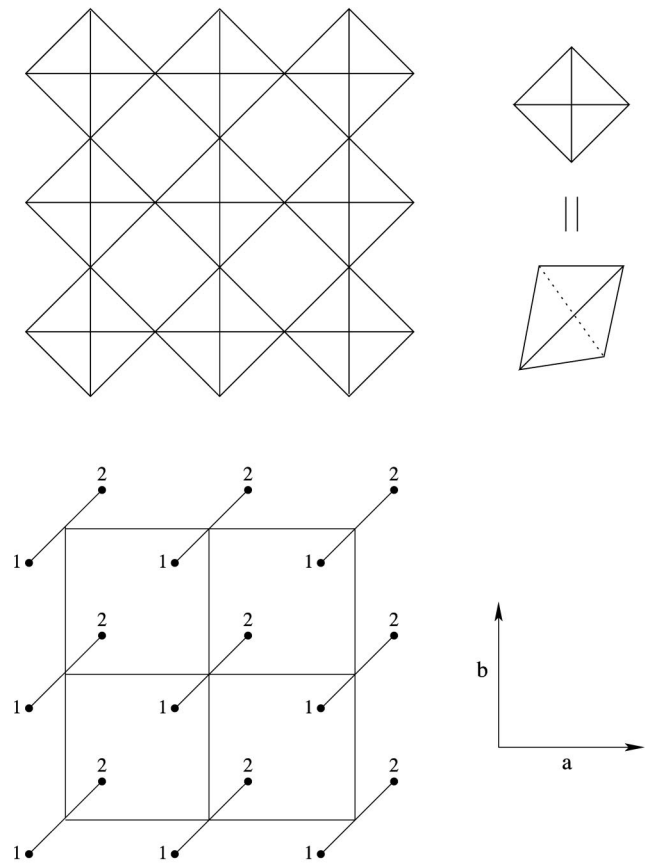

FIG. 1. The checkerboard lattice. It can be pictured as a square lattice of tetraheda (top). Locally, it reproduces the same environment as the three-dimensional pyrochlore lattice. In order to simplify our calculations, it has been described by a square lattice with a two-spin unit cell (bottom).
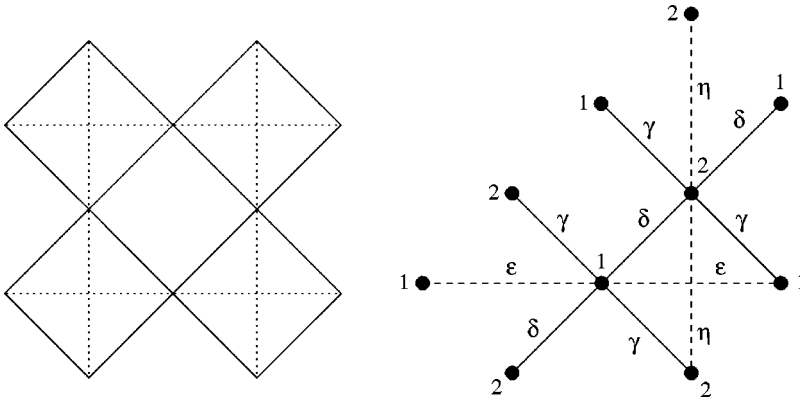
FIG. 2. (left) Lattice of coupling constants J and J'. Bold lines design constant J while dotted lines describe constant J'. (right) Local environment of a unit cell. $\vec{\delta}$ and $\vec{\gamma}$ are related to J-like coupling while $\vec{\epsilon}$ and $\vec{\eta}$ correspond to J'.

This system is two dimensional and can be described as the two-dimensional analog of the pyrochlore lattice: each atom possesses locally the same environment. It has recently been proved that its quantum ground states are singlets[10] for finite systems. The aim of this work is to test whether this conclusion is valid for an infinite lattice. To do so we start away from the isotropic checkerboard limit, when diagonal bonds are weakened (see Fig. 2), and we test whether this system undergoes a Neél ordering transition when reaching the isotropic limit. This approach is very close in spirit to the one previously done by Chandra and Douçot[11] on the J_1-J_2 square lattice model. This is done within the frame of linear spin-wave theory and the Dyson-Maleev approximation.[12] Whereas for the linear spin wave approach there always exists a critical coupling for which the local magnetization is unstable, whatever the value of the spin, in the case of the Dyson-Maleev approach there is a critical coupling only for the case $S = \frac{1}{2}$. The peculiar case $S = \frac{1}{2}$ is explored within a fermionic large-n limit of the SU(2) Hamiltonian. It is found that the system should order in a valence-bond solid of disconnected four-spin singlets. The notation, the Hamiltonian, and the linear spin-wave analysis are introduced in Sec. II. The Dyson-Maleev formalism is shortly described in Sec. III as it can be seen as an extension of Sec. II. Results of the linear spin-wave theory and the Dyson-Maleev approach are presented and discussed in Sec. IV. The case $S = \frac{1}{2}$ is detailed in Sec. V.

II. LATTICE, HAMILTONIAN, AND SPIN-WAVE ANALYSIS

A. Notation and lattice description

The checkerboard lattice can be described as a square lattice with a unit cell containing two spins (see Fig. 1). Each cell of the lattice can be obtained from the others by applying the translations $a = (1,0)$ and $b = (0,1)$. This means that each site of the lattice can be defined by two indices (i,n). The first corresponds to the unit cell $(i = 1, \ldots, N)$ where N is the total number of cells in the lattice and the other to the type of the site $(n = 1,2)$. We introduce two kinds of interactions J and J'. Here J corresponds to a coupling constant on a square lattice. J' can be seen as a coupling constant within one square over two of the square lattice (see Fig. 2). Using this notation, the Brillouin zone of the underlying Bravais lattice is $\mathrm{BZ}(k_x, k_y) = [-\pi, \pi] \times [-\pi, \pi]$ and the structure

coefficients can be defined as $\delta = \cos(\vec{k} \cdot \vec{\delta}) = \cos[(k_x + k_y)/2]$, $\gamma = \cos(\vec{k} \cdot \vec{\gamma}) = \cos[(k_x + k_y)/2]$, $\epsilon = \cos(\vec{k} \cdot \vec{\epsilon}) = \cos(k_x)$, and $\eta = \cos(\vec{k} \cdot \vec{\eta}) = \cos(k_y)$ where $\vec{\delta}$, $\vec{\gamma}$, $\vec{\epsilon}$, and $\vec{\eta}$ are depicted in Fig. 2.

B. Spin-wave Hamiltonian

The Heisenberg Hamiltonian for this system is

$$H = -\sum_{ij} J_{ij} S_i \cdot S_j, \tag{1}$$

where J_{ij} are coupling constants ($J_{ij} < 0$ for an antiferromagnet) and S_i is the spin located at site i. This spin Hamiltonian may be transformed into a boson Hamiltonian through an Holstein-Primakoff transformation, provided that we know its mean-field (MF) ground states from the square lattice limit to the checkerboard lattice limit, i.e., for all values of $r = J'/J$. One way to know the MF ground state(s) is to compute the Fourier transform of the interactions on the lattice:[13]

$$H = -\sum_{i,j} J_{ij} S_i \cdot S_j = \sum_q J(\vec{q}) S_{\vec{q}} \cdot S_{-\vec{q}}. \tag{2}$$

As we here deal with a two-spin unit cell, its Fourier transform $J(\vec{q})$ is a 2×2 matrix and must be diagonalized to find the normal modes $\lambda^{\mu = 1,2}(\vec{q})$. The ground state (if unique) then corresponds to the lowest eigenvalue $\lambda^1(\vec{q}_0)$ and is described by the propagation vector $\vec{q}_0$ and the associated eigenvector $V_1(\vec{q}_0)$ which fixes the inner structure of the unit cell. In the range $0 \leq r < 1$, $\vec{q}_0$ always equals 0 and the eigenvector is always equal to $(1, -1)$ which means that the ground state is nondegenerate and corresponds to the antiferromagnetic Néel state (see Fig. 3, top and middle). At the peculiar point $r = 1$, we obtain a flat branch, signaling that at the MF level, the system is continuously degenerate (see Fig. 3, bottom), as previously noted in Ref. 13. That behavior can be explained in terms of local degrees of freedom. In the limit $J' = J$, we note that the Hamiltonian may be decomposed as a sum of squares over "tetrahedra," as has been done in the *kagomé* as well as in the pyrochlore lattice:
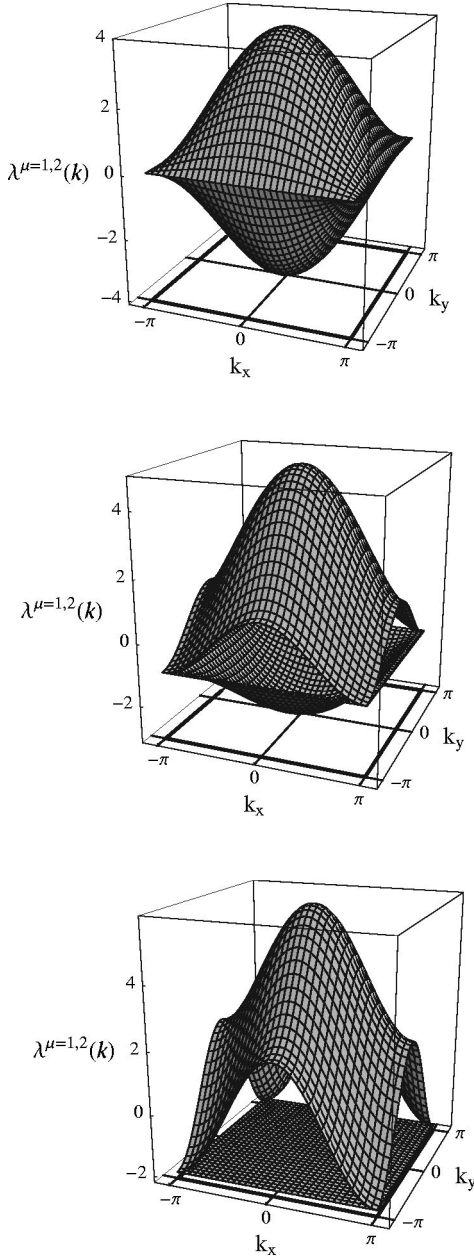
FIG. 3. Fourier transform of the interactions for the square lattice limit ($r=0$, top), an intermediate case ($r=0.5$, middle), and the checkerboard limit ($r=1$, bottom). Each manifold corresponds to an eigenvalue of $J(\vec{q})$.

$$H=-J\sum_{ij} S_i \cdot S_j = -\frac{J}{2}\sum_{\text{tet}} \left(\sum_{i=1}^{4} S_i\right)^2 + 2NJS(S+1).$$

(3)

We see that the classical ground state is defined by the constraint $\Sigma_{i=1}^{4}S_i=0$ on each tetrahedron. Furthermore, as tetrahedra are corner sharing, this constraint is not sufficient to order the system and there are an infinite number of ways to satisfy it, which results in a flat branch over the whole Brillouin zone. This is exactly the same phenomenon that was previously observed on the *kagomé* as well as on the pyrochlore lattice. Nevertheless, the Néel state belongs to this
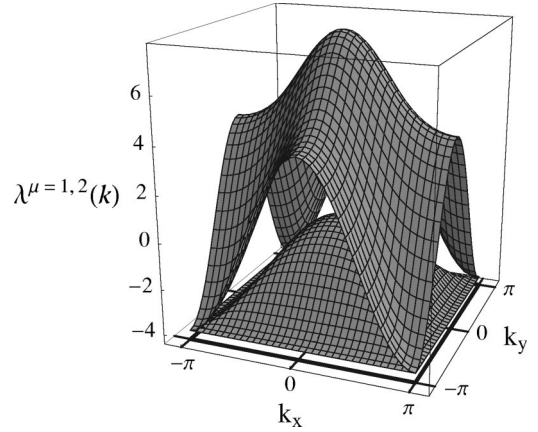

FIG. 4. Fourier transform of the interactions for $r=2$. Each manifold corresponds to an eigenvalue of $J(\vec{q})$. The mean-field ground state is continuously degenerate along lines which unable the choice of a trial ground state for the spin-wave analysis.

infinite set of MF ground states, and as it is the correct one for any $r<1$, we will also consider this state by continuity for the point $r=1$. For the parameter range $r>1$, the situation is quite different as MF ground states are continuously degenerate along lines corresponding to the border of the square lattice Brillouin zone (see Fig. 4). This precludes a description via a spin-wave analysis in this range as no magnetic ground state can be chosen as a trial state. This is the same situation as the one encountered on the *kagomé* or the pyrochlore lattices where spin-wave calculations can only compare the relative stability of Néel states without considering the entire set of these states.[14] So we will restrict ourselves to the range $0 \leqslant r \leqslant 1$ and consider the antiferromagnetic Néel state as the trial state. We therefore introduce two species of bosons, each one related to a different sublattice, and restrict the development of spin operators to the lowest order in the spin-wave expansion. The resulting bosonic Hamiltonian is then diagonalized through a Bogoliubov transformation. We are left with two branches of ''magnons'' whose dispersions are $\epsilon_\alpha=(1/2)[f-g+\sqrt{(f+g)^2-4h^2}]$ and $\epsilon_\beta=(1/2)[-(f-g)+\sqrt{(f+g)^2-4h^2}]$ where $f_k=2+r(\epsilon-1)$, $g_k=2+r(\eta-1)$, $h_k=\delta+\gamma$, and $r=J'/J$ (δ, γ, ϵ, and η are defined in Sec. II A).

Restricting ourselves to the ground state, the energy and the local magnetization are obtained through

$$E=\frac{1}{2N}H=2JS^2-J'S^2-JS\sum_{\vec{k}} \mathcal{C}(\vec{k}),$$

(4)

$$M=\langle S_i^{1z}\rangle_0 = S - \langle c_i^\dagger c_i\rangle_0 = S - \frac{1}{N}\sum_{\vec{k}} v_\alpha^2(\vec{k}),$$

(5)

with $\mathcal{C}_k = \frac{1}{2}[\epsilon_\alpha + \epsilon_\beta + (f-g)(u_\alpha^2 - u_\beta^2) - (f+g)]$ and where the coefficients of the Bogoliubov transformation are $u_\alpha = h/\sqrt{h^2-(\epsilon_\alpha-f)^2}$, $v_\alpha = (f-\epsilon_\alpha)/\sqrt{h^2-(\epsilon_\alpha+f)^2}$, $u_\beta = (\epsilon_\beta+f)/\sqrt{(\epsilon_\beta+f)^2-h^2}$, and $v_\beta = h/\sqrt{(\epsilon_\beta+f)^2-h^2}$.

III. DYSON-MALEEV REPRESENTATION

We use the same Hamiltonian of Eq. (1) and introduce the Dyson-Maleev transformation.[12] Because of its algebra, the Dyson-Maleev transformation rewrites the Hamiltonian of Eq. (1) as a sum of two and four operators terms. The simplest method to solve the problem is to decouple the four operators term introducing an *a priori* decoupling scheme. In the present case, we follow the mean-field decoupling of Ref. 15. Three quantities are introduced that correspond each to a two-boson-like excitation:

$$\mathcal{D} = \langle a_i^\dagger a_i \rangle = \langle b_j^\dagger b_j \rangle,$$

$$\mathcal{O} = \langle a_i^\dagger a_l \rangle = \langle b_j^\dagger b_m \rangle, \quad i \neq l, \quad j \neq m,$$

$$\mathcal{T} = \langle a_i^\dagger b_j^\dagger \rangle. \tag{6}$$

Other types of excitations are neglected and considered as higher-energy processes as previously proposed by Takahashi.[16] Using these approximations, the Dyson-Maleev Hamiltonian is then linearized and diagonalized through another Bogoliubov transformation. The structure of the transformation is identical to the one of the linear spin-wave case, but with new coefficients. These coefficients are $f'_k = 2A + rB(\epsilon - 1)$, $g'_k = 2A + rB(\eta - 1)$, and $h'_k = A(\delta + \gamma)$ where $A = 1 - (\mathcal{D} + \mathcal{O})/2S$ and $B = 1 - (\mathcal{D} - \mathcal{T})/2S$. Finally the three self-consistent coefficients at zero temperature are obtained through the three coupled relations

$$\mathcal{D} = \frac{1}{N} \sum_k v'^2_\alpha(k),$$

$$\mathcal{O} = -\frac{1}{2N} \sum_k u'_\alpha(k) v'_\alpha(k)(\delta + \gamma),$$

$$\mathcal{T} = \frac{1}{2N} \sum_k v'^2_\alpha(k)(\epsilon + \eta), \tag{7}$$

and the local magnetization of the Néel state is simply $M = \langle S_i^{1z} \rangle_0 = S - \mathcal{D}$.

IV. RESULTS OF THE SPIN-WAVE APPROACH

In the following, we fix $J = -1$ and take $-1 \leq J' \leq 0$. We first discuss the linear spin-wave (LSW) results and then the Dyson-Maleev approach. In Figs. 5 and 6, the energy as well as the local magnetization is plotted as functions of the ratio $r = J'/J$. For the case $r = 0$, well-known results for the $S = 1/2$ sqaure lattice are recovered: $E = -0.658$ and $M = 0.3$. The magnon spectrum is very simple; there is only one dispersive branch, which is two times degenerate in our case because of the two-spin unit cell description (Fig. 7, top). With increasing r, there are three zones to distinguish. First, in the range $0 \leq r \leq r_c$, the magnon spectrum has two distinct manifolds, each of these being dispersive (Fig. 7, middle). This occurs now because the sites of the unit cell no longer have the same symmetry. r_c corresponds to a critical coupling below which the local magnetization is finite, even renormalized by quantum corrections. For $S = 1/2$, $r_c \approx 0.75$,
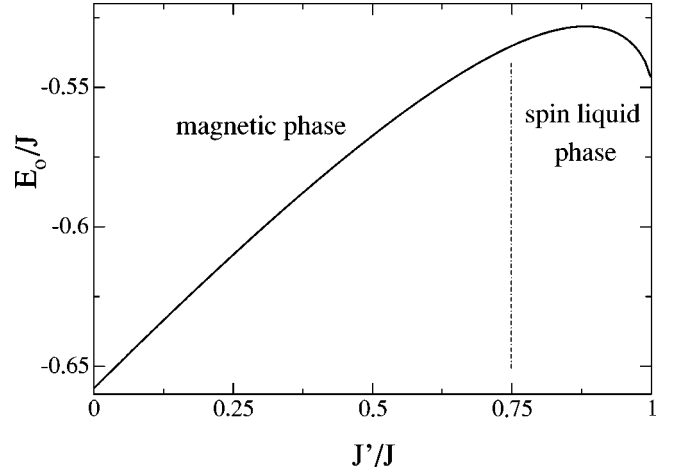

FIG. 5. Energy per site as a function of the ratio $r = J'/J$, i.e., between the limits of the square lattice and the checkerboard lattice, for $S = 1/2$. Beyond the critical ratio $r \approx 0.75$, the value of the energy is meaningless as it describes the energy of an unstable state.

which was already obtained in Ref. 17, and for $S = 1$, $r_c \approx 0.93$. Critical values for higher spins are shown in the phase diagram of Fig. 8. The second zone corresponds to the range $r_c \leq r < 1$. Because of quantum corrections, local magnetization is renormalized to zero, which means that in this approximation, the system does not show magnetic ordering. Even if quantum fluctuations drive the system to disorder, one notes that magnons are still dispersive. This means that there is no peculiar contribution coming from their structure. This is no longer the case for the special point $r = 1$. At this point, the lowest branch of spin waves is flat over the whole Brillouin zone (Fig. 7, bottom). This has several consequences. First, this means that at the level of this approximation, there will always be a critical coupling, whatever the value of the spin. This comes directly from the nonanalytic behavior of $v_\alpha(\vec{k})$ when $r \to 1$ along directions $ky = \pm kx$. Because of that, the local magnetization diverges as $-1/\sqrt{(1-r)}$, i.e., is renormalized to zero, whatever the value
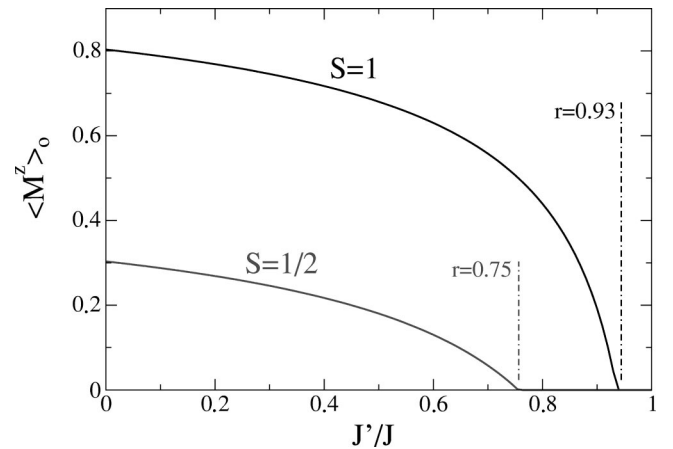

FIG. 6. Local magnetization as a function of the ratio $r = J'/J$, i.e., from the square lattice to the checkerboard lattice. Gray lines correspond to the calculations made for $S = 1/2$ and black lines for $S = 1$.
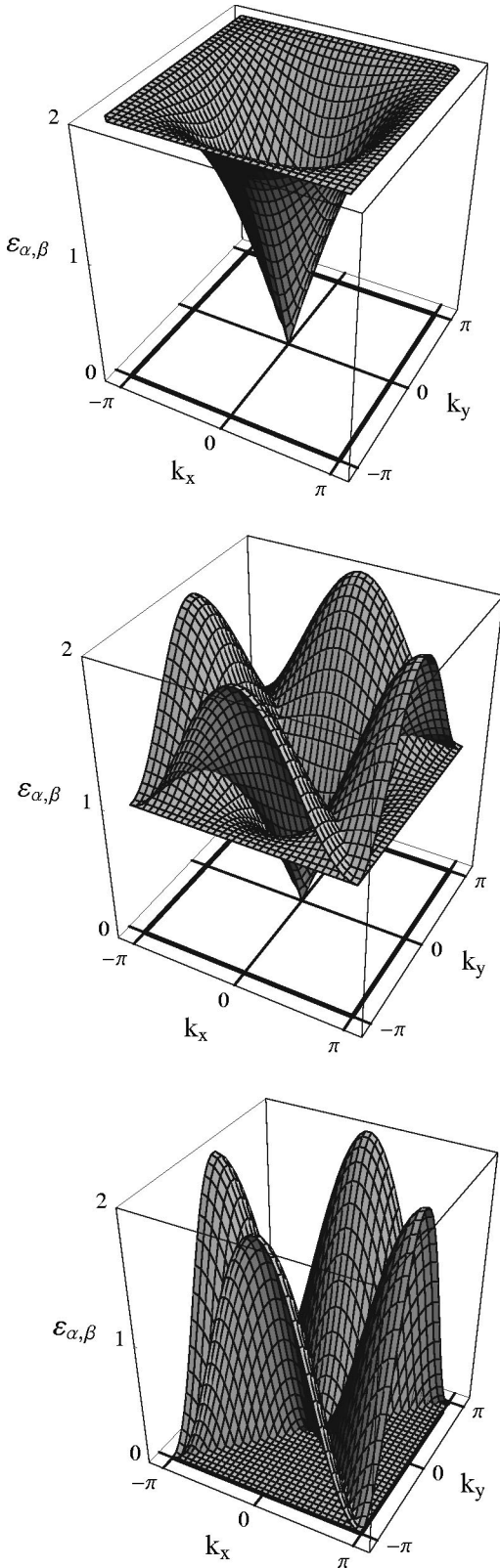
FIG. 8. Stability of the Neel state. The straight line indicates the threshold below wich the Neel state is stable for a given ratio $r = J'/J$. Over this line, it is destabilized by geometry and quantum fluctuations. For $r = 1$, it is always unstable, whatever the value of the spin S.

of S. Consequently, we obtain a phase diagram $(1/S, J'/J)$ very similar to the one of the J_1-J_2 square lattice model where J'/J plays the role of J_2/J_1 (see Fig. 8 and Fig. 2 of Ref. 11). This problem of a flat mode is often encountered in frustrated lattices and it rules out the possibility of studying the $r = 1$ point without going to the next order of expansion in our model, i.e., without including quartic terms. Whether such an inclusion of quartic terms is relevant is not clear as it corresponds to considering quartic modes as perturbations of *zero* quadratic modes. Nevertheless, it is the simplest next step to be done in the frame of spin-wave (Holstein-Primakoff) analysis.[14] Second, it has a meaning very close to the MF conclusions. If the lowest branch of the magnons is flat, this means that the system has no spin stiffness. Thus, any local deformation will not propagate through the lattice. This is very close to the argument of continuous degeneracy obtained through the MF approach, i.e., the existence of an infinite number of local degrees of freedom [see Eq. (3)]. These degrees of freedom are one of the signatures of frustrated systems and may be counted, in the case of classical spins, through the ''Maxwellian counting'' rule.[7] At the level of the LSW approximation, this means that quantum fluctuations and geometrical frustration may destabilize the Néel state for a finite range of J'. Wether a quantum spin-liquid ground state in this range is stable is beyond this approach even if the existence of critical couplings goes in the right direction.

We now turn to the Dyson-Maleev approach. As for the preceding case, the local magnetization has been computed for different value of the spin. The main result is that for all $S \geq 1$, there is no critical coupling; i.e., the local magnetization of the Néel state is always finite in the isotropic limit $r = 1$. This is illustrated in Fig. 9 where reduced local magnetization $\langle S_i^z \rangle_0 / S$ is plotted versus the inverse spin value $1/S$ at $r \to 1$. The only exception is for $S = \frac{1}{2}$ for which it seems that there is a critical coupling at $r \approx 0.98$. To test whether the stability of the Néel state for the $S = \frac{1}{2}$ comes

FIG. 7. Magnons dispersions $\epsilon_{\alpha,\beta}(k)$ over the Brillouin zone. From top to bottom, $r = 0, 0.5, 1$. At $r = 1$, the lowest branch is non-dispersive. This means that this point is remarkable and reveals (as in the *kagomé* and pyrochlore lattice cases) the presence of a soft mode related to local degrees of freedom.
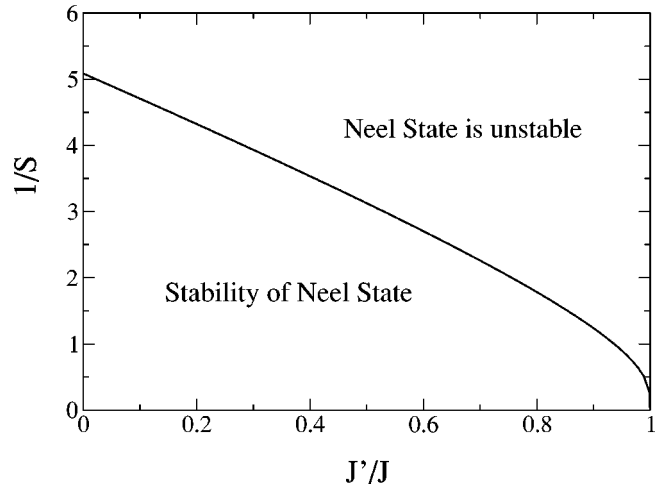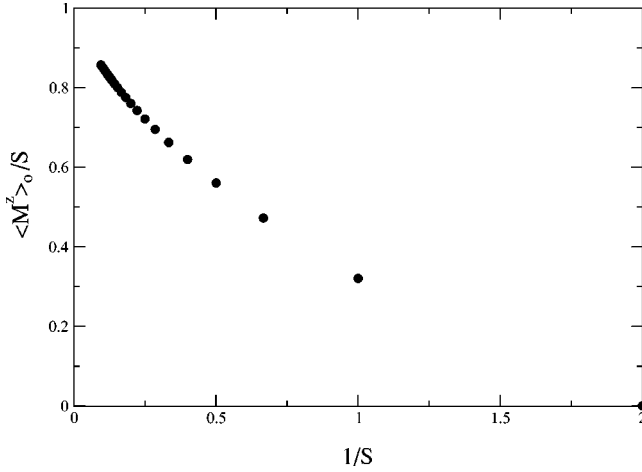
FIG. 9. Relative local magnetization of the Néel state vs the inverse spin value $1/S$ at the isotropic point. For all $S \geq 1$, the local magnetization is finite, suggesting that the ground state could be the Néel state. For $S = 1/2$, the local magnetization is renormalized to zero by quantum fluctuations.

from a flat mode or from quantum fluctuations, we have plotted the associated dispersions over the whole Brillouin zone (see Fig. 10). From the structure of the boson excitations, it is clear that including quantum fluctuations via the Dyson-Maleev formalism destroys the pathological structure of the flat mode. Therefore, destabilization of the Néel state is only driven by quantum fluctuations within this approxi-
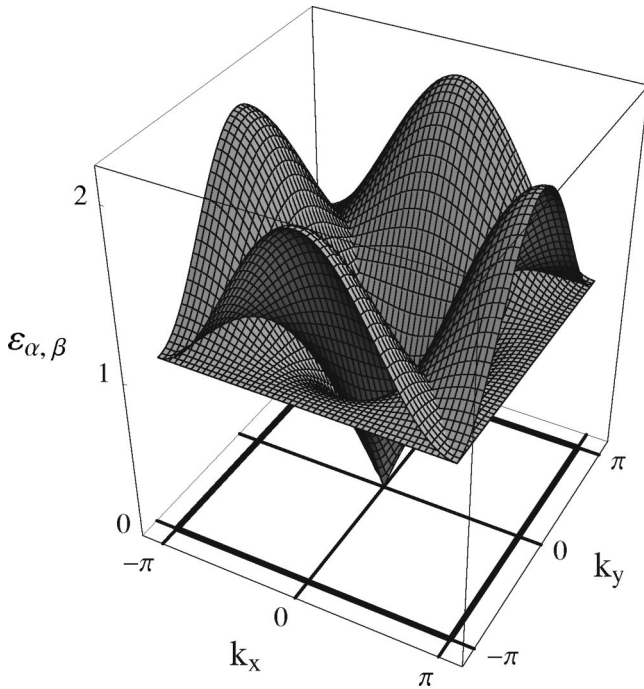

FIG. 10. Energy dispersions corresponding to the boson excitations around the Néel state for the $S = 1/2$ case in the limit $r \to 1$. The dispersions are no longer pathological as they are in the LSW approximation and the flat mode is destroyed. This clearly indicates that destabilization of the Néel state is driven here only by quantum fluctuations.

mation and not by a zero spin stiffness as was the case in the LSW approximation in the limit $r \to 1$.

These results are quite surprising as they are qualitatively different from the LSW approximation. This suggests that the more accurately the quantum fluctuations are taken into account, the more the Néel state is stable, even in the isotropic limit. This is unexpected as the checkerboard antiferromagnet was expected to behave like the *kagomé* antiferromagnet. In the latter case, the reduction of the local magnetization to zero by quantum fluctuations and geometry, within a finite range of couplings, has been shown using two distinct numerical methods.[18] It was found that going from the triangular limit to the *kagomé* limit, there is a singular point associated with a critical coupling ($r_c = J'_c/J \approx 0.9$), where local magnetization vanishes. Here, we obtain the same conclusion within the LSW approximation but not within the mean-field treatment of the Dyson-Maleev (DM) approach. Whether this discrepency comes from the quantum fluctuations that are better incorporated into the latter formalism or comes from the mean-field treatment of the DM representation is not clear. Nevertheless, it is interesting to note that a recent work[19] shows the same tendency, i.e., a transition from an $S = 0$ ground state to a stable Néel state with increasing spin size S. If the present calculations treat correctly quantum fluctuations (which is not proved in this paper), the frontier between the expected valence-bond solid (VBS) and Néel ordering[19] would then be at $S = 1$. Nevertheless, it should be stressed that the present work does not test whether other classical ground states could be stable at the isotropic point and have the same or a different energy than the Néel ground state. Consequently, an intrinsic or accidental degeneracy of magnetic ground states for $S \geq 1$ is not ruled out by this approach.

V. $S = 1/2$ CASE

As shown in the preceding sections, it seems that only for $S = 1/2$ can the ground state be nonmagnetic. To shed light on the behavior of the $S = 1/2$ checkerboard antiferromagnet, it is possible to use a "fermionic" $SU(n)$ generalization of the $SU(2)$ group. [Note that $n > 2$ does not correspond to a higher-spin representation of $SU(2)$. Therefore, a mean-field solution of the $SU(n)$ Hamiltonian is expected to be much closer to the $SU(2)$ physics than the classical description of Sec. II B.] This formalism has been previously introduced by Marston and Affleck[20] and applied to the square antiferromagnet. The advantage of this description is that it works on all lattices, even frustrated[21] or not bipartite, and that it is well suited for the checkerboard antiferromagnet as spin order never occurs in the exactly solvable large-n limit,[20] as is expected in the range $r_c \leq r \leq 1$ for $n = 2$. At large n, the Hamiltonian can be written as

$$H = \sum_{(i,j)} \left\{ \left(\frac{n}{J}\right) |\chi_{ij}|^2 + \sum_{\alpha=1}^{n} (\chi_{ij} c_{i\alpha}^\dagger c_{j\alpha} + \text{H.c.}) \right\}, \quad (8)$$

where $\chi_{ij} = (J/n) c_{i\alpha}^\dagger c_{j\alpha}$ are bond variables and where the spin-spin interaction has been expressed by use of electron operators through $S_i \cdot S_j = (1/2) \Sigma_{\alpha,\beta} c_{i\alpha}^\dagger c_{j\beta} c_{j\beta}^\dagger c_{j\alpha} + \text{const.}$
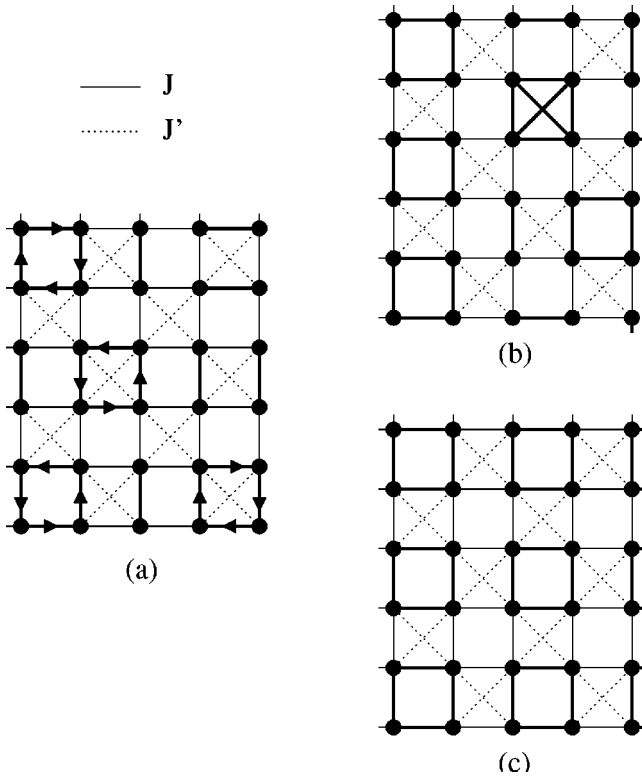
FIG. 11. (a) General box phase on the J square lattice of the anisotropic checkerboard antiferromagnet (as shown in Fig. 4 of Ref. 24). Bold lines without arrows correspond to nonzero χ_{ij} while thin lines, plain or dashed, correspond to $\chi_{ij}=0$. Bold lines with arrows indicate that $\chi_{ij}=\chi e^{i\pi/4}$ where χ is real. The product of χ_{ij} around each box is negative, indicating a flux of π. These boxes are the large-n equivalent of a four-spin singlet on a square. (b) Picture of a general box phase for the $S=1/2$ case. Bold squares correspond to four-spin singlets and bold lines to two-spin singlets. If J' inter-actions are within a box, they must be taken into account and are also in bold as they enter the calculation of the energy. The different energies for squares with crossings, squares without crossings, and links are, respectively, $E=-1.5$, $E=-2$, and $E=-0.75$. (c) Picture of the valence-bond solid for the $S=1/2$ case, expected to be the ground state. This state is two times degenerate and involves only squares without crossings.

The χ variables may be seen as valence-bond operators[22] as $(n/J)\chi_{ij}^{\dagger}\chi_{ij}$ is the number of valence bonds on the link (ij). Therefore, in this formalism, every ground state is described by a map of these complex scalar fields. Several authors have concentrated on the mean-field solutions ("$1/n=0$"),[20,23,24] and in particular, it is possible to apply here a theorem established by Rokhsar.[24] First, it is clear that the checkerboard antiferromagnet is "dimerizable with respect to J" as "it is possible to partition the network into disjoint pairs of sites such that (a) every site belongs to one and only one pair and (b) for each pair (i,j) we have $J_{ij}=J$." In the range $J \gg J'$ it is possible to apply his theorem which shows that mean-field ground states are (spin-Peierls or box) phases[24] (see Fig. 11). Keeping in mind that the case of interest is for $n=2$, we look for the proposed states that lower the energy of the real $S=1/2$ case. It is straightforward to see that box phases lower this energy with respect to J, as soon as these phases are

regular tilings of the underlying square lattice by disconnected J squares (see Fig. 11). Taking now into account the J' couplings, only one of these phases survives, where J' links are not frustrated. At this point, it means that *if* the SU(n) description of the SU(2) case is relevant, it suggests that for $S=1/2$, in the range $r_c \leq r \leq 1$, the ground state should be two times degenerate (because there are two choices for the tiling), consisting in a valence-bond solid of disconnected squares without crossings (in the range $0 \leq r < r_c$ it is clear that this formalism is not relevant as the local magnetization is finite). The proposed ground state [see Fig. 11(c)] could be tested by comparing the VBS energy per site, $E=-0.5$, and the correlations functions with results of exact diagonalizations, for example.[25]

VI. DISCUSSION AND CONCLUSION

To conclude, linear spin-wave analysis has shown that away from the isotropic checkerboard lattice limit, there is a finite range of coupling for which the Néel state is unstable, whatever the value of the spin. Strikingly, when using a self-consistent decoupling within the Dyson-Maleev formalism, it is shown that the Néel state is never destabilized, except for the $S=\frac{1}{2}$ case. The stability of the Néel state with respect to other magnetized states has not been tested in this work. Recent work[19] supports that this state should be the ground state for large S. It is compatible with the present results, although it is at variance with results obtained with the infinite-component[26] antiferromagnetic model on the checkerboard lattice ($d\rightarrow\infty$). A possible explanation for this[27] is that for large S, there should be quantum order by disorder (as supported in Ref. 19) but this order by disorder comes with an energy scale of J/S rather than J. Therefore, in the classical limit, the temperature at which the correlation length grows exponentially goes to zero. In other words, the limits $T\rightarrow0$ and $S\rightarrow\infty$ (or $d\rightarrow\infty$) should not commute. For the special $S=\frac{1}{2}$ case, the fermionic large-n limit suggests that the ground state is a valence-bond solid of disconnected four-spin singlets on squares without crossings. That conclusion is consitent with results of Refs. 19 and 25.

The present work shows that the isotropic checkerboard antiferromagnet should display behaviors qualitatively different from the one of the *kagomé* and the pyrochlore antiferromagnet. Moreover, quantum fluctuations have to be treated with care as they can drive the system from a purely quantum ground state to a Néel-like ground state. In this frame, the structure of the singlet and triplet towers of state should be extremally S dependent and exact diagonalization of finite clusters with different spin size would be of high interest, especially to test whether the descrepency already appears between the $S=\frac{1}{2}$ and the $S=1$ cases.

Note added in proof. After submission of the present paper, we have learned about a related work by Brenig *et al.*[28]

*Electronic address: canals@polycnrs-gre.fr; URL: http://ln-w3.polycnrs-gre.fr/pageperso/canals/

[1] F. D. M. Haldane, Phys. Lett. **93A**, 464 (1983).

[2] G. H. Wannier, Phys. Rev. **79**, 357 (1950).

[3] R. M. F. Houtappel, Physica (Amsterdam) **16**, 425 (1950).

[4] E. H. Lieb and D. Mattis, J. Math. Phys. **3**, 749 (1962).

[5] P. Lecheminant, B. Bernu, C. Lhuillier, L. Pierre, and P. Sindzingre, Phys. Rev. B **56**, 2521 (1997).

[6] D. A. Garanin and B. Canals, Phys. Rev. B **59**, 443 (1999).

[7] R. Moessner and J. T. Chalker, Phys. Rev. Lett. **80**, 2929 (1998); Phys. Rev. B **58**, 12 049 (1998); R. Moessner, Ph.D. thesis, Oxford University, 1996.

[8] B. Canals and C. Lacroix, Phys. Rev. Lett. **80**, 2933 (1998); Phys. Rev. B **61**, 1149 (2000).

[9] For a collection of articles, see *Magnetic systems with Competing Interactions: Frustated Spin System*, edited by H. T. Diep (World Scientific, Singapore, 1994); for Ising systems, see R. Liebmann, *Statistical Mechanics of Periodic Frustrated Ising Systems* (Springer, Berlin, 1986); see reviews, see A. P. Ramirez, Annu. Rev. Mater. Sci. **24**, 453 (1994); P. Schiffer and A. P. Ramirez, Comments Condens. Matter Phys. **18**, 21 (1996); M. J. Harris and M. P. Zinkin, Mod. Phys. Lett. B **10**, 417 (1996).

[10] E. H. Lieb and P. Schupp, Phys. Rev. Lett. **83**, 5362 (1999).

[11] P. Chandra and B. Douçot, Phys. Rev. B **38**, 9335 (1988).

[12] F. J. Dyson, Phys. Rev. **102**, 1217 (1956); **102**, 1230 (1956); S. V. Maleev, Zh. Éksp. Teor. Fiz. **30**, 1010 (1957) [Sov. Phys. JETP **6**, 776 (1958)].

[13] E. F. Bertaut, in *Spin Arrangement and Crystal Structure, Domains and Micromagnets*, edited by T. Rado and H. Suhl (Academic Press, New York, 1963), Vol. III; J. N. Reimers, A. J. Berlinsky, and A.-C. Shi, Phys. Rev. B **43**, 865 (1991).

[14] A. Chubukov, Phys. Rev. Lett. **69**, 832 (1992).

[15] D. Chu and J. L. Shen, Phys. Rev. B **44**, 4689 (1991).

[16] M. Takahashi, Phys. Rev. B **40**, 2494 (1989).

[17] R. R. P. Singh, O. A. Starykh, and P. J. Freitas, J. Appl. Phys. **83**, 7387 (1998).

[18] D. J. J. Farnell, R. F. Bishop, and K. A. Gernoth, Phys. Rev. B **63**, 220402 (2001); C. Waldtmann and P. Lecheminant (unpublished).

[19] R. Moessner, Oleg Tchernyshyov, and S. L. Sondhi, cond-mat/0106288 (unpublished).

[20] J. B. Marston and I. Affleck, Phys. Rev. B **39**, 11 538 (1989).

[21] J. B. Marston and C. Zeng, J. Appl. Phys. **69**, 5962 (1991).

[22] Ian Affleck and J. Brad Marston, Phys. Rev. B **37**, 3774 (1988).

[23] Thierry Dombre and Gabriel Kotliar, Phys. Rev. B **39**, 855 (1989).

[24] Daniel S. Rokhsar, Phys. Rev. B **42**, 2526 (1990).

[25] J.-B. Fouet, M. Mambrini, P. Sindzingre, and C. Lhuillier, cond-mat/0108070 (unpublished).

[26] B. Canals and D. A. Garanin, cond-mat/0102235, Eur. Phys. J. B (to be published).

[27] R. Moessner (private communication).

[28] W. Brenig and A. Honecker, Phys. Rev. B **65**, 140407 (2002).